

Osama Mawlawi, Richard Wendt III,
and Wai-Hoi Gary Wong

Preamble

In the decade since the previous edition of this chapter was written, positron emission tomography (PET) and more recently PET/computed tomography (CT), has continued to grow in prominence within the field of nuclear medicine imaging. Surveys conducted by the market research firm IVM (Greenbelt, MD) show an average annual increase of 10.4% in the number of PET and PET/CT studies performed between 2005 and 2008 [1]. The trend, however, has seen a decline in more recent years. The advantages of PET/CT over dedicated PET imaging (described below) have also drastically changed the characteristics of the scanner models that are available from manufacturers. As of the middle of the first decade of 2000, none of the three principal manufacturers of PET scanners (GE Healthcare, Siemens Medical Solutions, and Philips Medical Systems), still offered a dedicated PET system;

O. Mawlawi, Ph.D. (✉) • R. Wendt III, Ph.D.
Department of Imaging Physics, The University of Texas
MD Anderson Cancer Center, Houston, TX 77030, USA
e-mail: omawlawi@mdanderson.org;
rwendt@mdanderson.org

W.-H.G. Wong, Ph.D.
Department of Experimental Diagnostic Imaging,
The University of Texas MD Anderson Cancer Center,
Houston, TX 77030, USA
e-mail: gwong@mdanderson.org

only hybrid PET/CT systems were being manufactured.

As we predicted in the first publication of this book chapter, the majority of PET/CT disadvantages – high density media such as intravenous or oral contrast, mismatch between PET and CT as a result of respiratory motion, and truncation resulting from differences in the size of the field of view between PET and CT – have been mitigated through the development of hardware and software solutions. A brief description of these solutions is provided under the “Challenges of PET/CT Imaging” subsection.

The advances in PET/CT imaging that have occurred since the first publication of this book chapter have resulted in a dramatic improvement in PET image quality. Examples of these advances include: higher sensitivity through the use of 3D imaging and longer axial fields of view (FOVs), accurate modeling of the imaging chain in fully 3D iterative reconstruction techniques, higher light output and shorter decay time with new detectors, higher image contrast with time of flight imaging, and finally richer image fusion through the emergence of PET/magnetic resonance imaging (MRI) as a new hybrid modality. A description of each of these advances is included in the section “Recent Advances in PET Imaging.”

Finally, the section titled “PET/CT Scanner Designs” has been updated to include the current commercially available systems from the three main manufacturers of PET/CT systems.

Introduction

In the past decade PET has emerged as a unique imaging modality with applications in cardiology, neurology, oncology, and psychiatry. It is unique among medical imaging methods in its ability to produce accurately quantifiable images of physiologic information, whereas other imaging techniques excel in their depiction of anatomic structures or their ability to image rapidly moving structures. The quantitative advantage of PET, coupled with the extended PET reimbursement by the major insurance carriers in the United States for a range of PET oncology studies, has further fueled the rapid increase in the clinical demand for this imaging modality. In this regard, research groups and industry have striven to optimize this imaging technique. One of the most recent developments in PET imaging has been the introduction of a combined PET/CT scanner. This chapter presents the reasons for this development. It discusses the advantages and artifacts presented by such imaging systems, the impact of PET/CT on patient management, and its applications in other areas such as radiation treatment planning.

PET Imaging and Its Disadvantages

PET is a noninvasive, diagnostic imaging technique for measuring the Accumulation of radiotracer in the human body. The majority of PET imaging has been performed in the field of oncology, where a whole-body PET scan using the radiolabeled glucose analog fluorodeoxyglucose (FDG) plays an important role in the diagnosis and management of cancer. FDG accumulation detected by PET has been shown to be a reliable method for accessing the glucose metabolic rate of human cells [2, 3]. Given that many malignant cells exhibit elevated glucose metabolism [4], FDG-PET has been used in the primary staging and therapeutic monitoring of cancer. The high sensitivity, specificity, and accuracy

of FDG-PET in detecting cancer in different regions of the body have been the driving forces behind its widening use [5, 6]. PET imaging however suffers from several drawbacks such as: 1) high noise content in attenuation correction factors, 2) long scan duration, and 3) lack of anatomical landmarks. These drawbacks are further described in the next sections and are the main motivation for the development of PET/CT systems.

Transmission Scan and Attenuation Correction

In a whole-body FDG scan, the patient receives the radiopharmaceutical as an intravenous injection and then rests quietly for about one hour while the FDG distributes within the body. Following this waiting period, the patient is moved to the scanner and lies supine on the patient couch. The patient is then positioned within the field of view of the scanner and the imaging session is initiated. A PET scan is composed of an emission scan and a transmission scan. The emission scan is used to depict the distribution of the radiopharmaceutical in the body (Fig. 3.1a), while the transmission scan is used for attenuation correction of the emission data. In ordinary PET, patient attenuation is measured by rotating radioactive sources around the patient while the detectors that surround the patient collect the transmitted annihilation photons – hence the term *transmission scan*. The transmission scan is used to compute a map representing the linear attenuation coefficients of different tissue types at the corresponding anatomic locations in a manner similar to x-ray CT but with poorer image resolution and quality (Fig. 3.1b). Multiplying the emission scan by the attenuation correction map generates the final, corrected PET image (Fig. 3.1c). Accurate attenuation correction is a major advantage of PET over other nuclear medicine imaging techniques. Corrected PET images depict an accurate distribution of the injected activity with minimal distortion in the shape, size, and location of a lesion. The value of

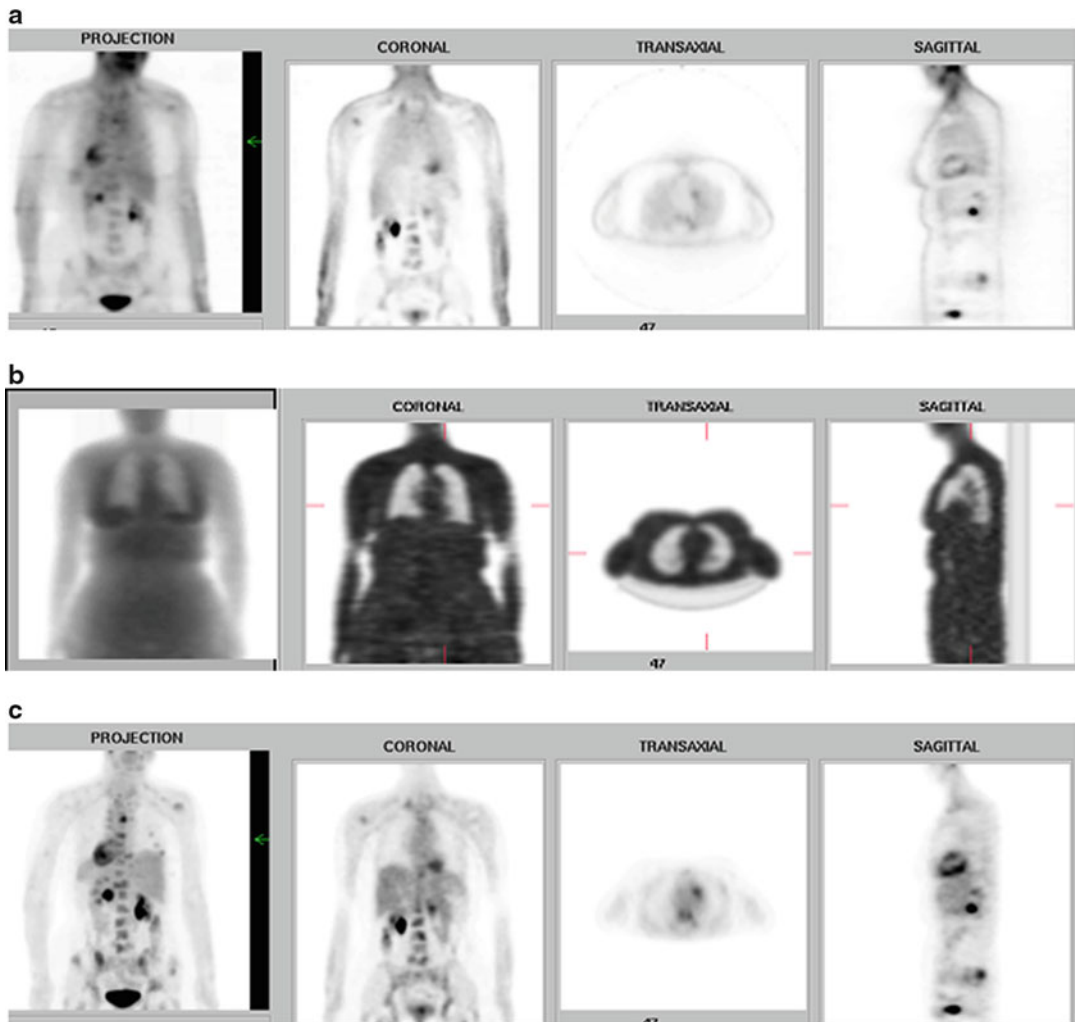


Fig. 3.1 (a) Nonattenuation corrected PET images; (b) reconstructed attenuation PET images; (c) attenuation corrected PET images

attenuation correction is further increased when it can be performed reliably and accurately with minimal inconvenience to the patient [7].

Historically, transmission scans have been obtained before the acquisition of the emission data. The time that it takes for the FDG to distribute in the patient (about an hour), and the requirement for exactly the same patient positioning for the acquisition of both the emission and the transmission data necessitated that the emission and transmission data be acquired consecutively

without any time lapse. However, this produces transmission scans that are inherently contaminated by emission data. Such cross talk results in underestimated attenuation coefficients that can lead to inaccurate quantification of PET images [8]. Additionally, transmission scans using a rotating radioactive source are noisy as a result of the low gamma-ray flux of the radioactive source. The noisy data result in noisy attenuation coefficients. The propagation of that noise into the final, corrected image decreases the apparent

lesion contrast and reduces the detectability of small lesions in the final image.

Several techniques have been proposed and implemented in routine clinical settings to correct these transmission scanning drawbacks [9]. For emission contamination, transmission windowing and/or transmission image segmentation are in use currently. Windowing restricts the accepted coincident events only to those compatible with the instantaneous location of the radioactive source as it is rotating around the patient and rejects the emission data in which the line of response could not physically have included the transmission source, which reduces much of the emission contamination in the acquired transmission data. Transmission segmentation, on the other hand, restricts the reconstructed transmission scan to a predefined number of tissue types (typically air, water, bone) that are based on a preset range of attenuation values. Each segment is then filled with a constant attenuation value that is characteristic of that tissue type [10, 11]. Transmission segmentation also significantly reduces the noise in the attenuation correction, thereby yielding a higher signal-to-noise ratio in the final, corrected images. Although these techniques have minimized the effects of emission contamination and noise, transmission segmentation results in an attenuation map composed of only the predetermined tissue types. Segmented transmission scans ignore the intermediate tissue densities in the patient [11], such as when a segment or voxel contains more than one tissue type. Noise in the transmission scan can also be reduced by acquiring transmission data for a longer period of time or by using higher radioactivity transmission sources. Both of these techniques, however, have drawbacks. A longer transmission scan time results in a higher probability of patient motion during the scanning session which reduces the spatial accuracy of the transmission image, and increases the inconvenience to the patient. A higher radioactivity source on the other hand, results in larger detector dead time and less accuracy in determining the attenuation factors.

PET Scan Duration

The acquisition of a transmission and emission scan to generate a corrected PET image requires a relatively long imaging session, particularly when whole-body scans are performed. Because the axial field of view of current PET scanners is only 15–17 cm, several pairs of emission and transmission scans (typically 5–7 in number) are needed to cover the whole height of a patient to obtain a whole body scan. Clinical studies have shown that the optimum scan duration per axial field of view (often called a “bed position”) is in the range of 3–5 min for the acquisition of the emission data and 2–3 min for the acquisition of the transmission data. The ranges reflect differences among scanners and the effect of the girth of the patient. This translates into a total scanning time of 25–60 min (of which 10–20 min is for transmission data), during which the patient should remain motionless to minimize the mismatch between the emission and transmission data, as well as to reduce image blurring. Such a scanning paradigm is inconvenient and uncomfortable for the patient. Furthermore, the PET scanner could output more (i.e., scan more patients in a day) if each patient’s examination took less time.

The challenge lies in the compromise among the competing demands of increasing the accuracy of attenuation correction by, lowering the noise propagated into the final image by this process, minimizing the mismatch between the true and measured attenuation maps, and minimizing the scanning time for maximum patient throughput. Ideally, attenuation correction would add little to the overall scanning time, giving it a negligible effect on patient throughput, and there would be essentially no noise and no segmentation errors propagated into the final attenuation-corrected image. These requirements, contrasted with the current state of attenuation correction, have led some clinics to skip transmission scanning altogether and to rely on images that have not been corrected for attenuation for their clinical evaluation of patients. The benefit of eliminating the lengthy transmission scan is argued to by far outweigh the gain

from accurate depiction of activity concentration [12, 13]. However, the clinical importance of quantitative PET, especially with accurate mapping to the patient's anatomy, as described in this book, would contradict this argument and bolster the case for attenuation correction for the sake of good care of the patient.

Image Registration and Fusion

Following the acquisition, attenuation correction, and reconstruction of PET data, the images are displayed for clinical evaluation. Regions of interest are usually drawn around areas of relatively high activity concentration, and an outcome measure such as the standardized uptake value (SUV) is reported. A major difficulty for the precise interpretation of PET scans is the absence of anatomic structures. PET images are characterized by lower resolution and are imprecise in their anatomic localization of foci of abnormal uptake. The accurate anatomic localization of a lesion coupled with its activity concentration can be important information that can be used in the diagnosis, staging, and treatment of patients. The usefulness of fusing functional PET data with anatomic information from CT or MRI has been recognized in oncology [14–17]. It has been shown that the visual correlation of PET with CT can improve the accuracy of interpretation over that using PET alone [18]. Traditionally, image registration and fusion have been performed through the use of computer algorithms. Before the advent of the hybrid PET/CT scanner, two image sets acquired from two different imaging modalities at two different times would be analyzed by the registration algorithms, and a mathematical transformation that would align one image set with the other would be generated. One of the major difficulties with the registration of images acquired at different times, and perhaps for different primary purposes, is the different patient positioning between the two image sets. Although this difficulty is minimal when registering images of rigid bodies such as the brain [19], its effect on aligning whole-body images, wherein the internal organs are nonstationary and

deformable, has resulted in less satisfactory registrations. For whole-body images, nonlinear image warping algorithms are needed; however, these algorithms require additional time to compute and are not always successful at aligning the two images, making their use less attractive in routine clinical PET imaging. Mental registration between PET and CT/MR images is usually performed by image readers. Such mental image registrations have, in the past, met the needs of experienced readers.

Advantages of PET/CT

To further improve PET imaging, the combined PET/CT scanner has been developed. CT measures the photon attenuation of the object being imaged, albeit at different electromagnetic energies than that used in PET. Mapping the CT attenuation coefficients corresponding to the different tissue types obtained at the CT equivalent energy to that of PET (511 keV) generates an attenuation correction map without the need to acquire a separate transmission scan [20]. CT images that have been acquired following FDG injection are less contaminated by emission data than are the source-based transmission scans described above. This is because of the large difference in flux (i.e., photons per second) between the CT x-rays and the emission gamma rays. In addition, CT images are characterized by shorter acquisition time and lower noise content than transmission images. This latter characteristic is dependent on the x-ray current setting of the CT scanner. The brief duration of CT scans occupies a small fraction of the overall time to scan a patient. Shortening the time that a patient must hold motionless reduces the discomfort of the examination for a patient and lessens the likelihood that a patient will move. Finally, CT images provide high-resolution anatomic information, which, when combined with PET images, can improve diagnostic accuracy and patient management [21–26].

Patient scheduling and radiation treatment planning are additional areas that benefit from PET/CT. Most patients who are scheduled for a

PET scan also receive a diagnostic CT scan prior to or after their PET imaging session [27]. These separate scans could be performed on the same PET/CT scanner in one extended session, thus facilitating patient scheduling and eliminating the need for transportation of the patient from one imaging suite to another. Patient waiting time would be reduced and throughput would improve. For radiation treatment planning, it has been shown that incorporating PET data into treatment planning along with CT has the potential to improve the accuracy of delineating the primary target volume [28–30]. Obtaining the PET and the CT data as a registered dataset greatly facilitates using the PET data in planning the treatment.

Challenges of PET/CT Imaging

Although combining a PET and a CT scanner has many advantages, this hybrid imaging system also presents a new set of difficulties, most of which are in regard to the use of CT for attenuation correction of the PET data. One of the major areas of difficulty is the presence of dense material such as dental fillings, metallic prostheses, and contrast agents within the field of view of the CT image. In the case of dental fillings and metallic prostheses, the resulting CT images are characterized by pronounced streaking artifacts as a result of the very high attenuation values. These artifacts are propagated into the PET image upon mapping the CT attenuation values to those corresponding to PET at 511 keV [31]. The propagated artifacts are manifested as high attenuation correction factors, which result in an artifactual increase in the apparent tracer concentration in the PET image [32]. For contrast agents, whether oral (barium sulfate) or intravenous (iodine), the overestimation of the attenuation correction factor presents an even more complicated challenge because the overestimation is dependent on the concentration of the administered contrast agent. The concentration of contrast agents in the body is not a fixed amount, but varies depending on several factors such as patient size, clearance, blood flow, and most importantly, the interval of

time between the administration of the contrast agent and the acquisition of the CT. It has been shown that both oral and intravascular contrast agents affect the quantitative and qualitative accuracy of PET images depending on the contrast concentration [33–37].

In the case of contrast media, whether oral or intravenous, these effects have been minimized on current PET/CT scanners through the use of modified transformations from CT numbers to PET attenuation values. Figure 3.2 shows the standard bilinear transformation used to map CT numbers to PET attenuation values. The same graph also shows other transformations for different CT kVp settings that are used when an oral or intravenous contrast agent is present in the CT image. At the onset of a PET/CT scan, the operator of the scanner presses a button to indicate whether the patient has oral or intravenous contrast. This in turn selects the appropriate transformation based on the CT kVp setting and reduces any artificial increase in PET attenuation coefficients because of a corresponding increase in CT number. PET/CT scanners from all manufacturers are currently equipped with a similar approach to minimize the effect of oral or intravenous contrast. Extending this technique to handle the effects of other high-Z materials is an ongoing endeavor.

Another complication of replacing the transmission scan with a CT scan is the attenuation artifact induced by the patient respiration. The CT scans are characterized by short duration and may be acquired during any phase of the patient's respiratory cycle. The PET scans, on the other hand, require longer imaging times and therefore are acquired over multiple respiratory cycles. Thus, images from the two scanning modalities might show discrepancies in the anatomic locations of various organs. This is particularly evident in the areas that are the most affected by respiration such as the dome of the liver and the base of the lungs. Because the CT images are used for attenuation correction of the PET emission data, the mismatch between the two image sets results in large quantitative and qualitative errors in the corrected PET images [38–41]. It has been shown, however, that by acquiring the

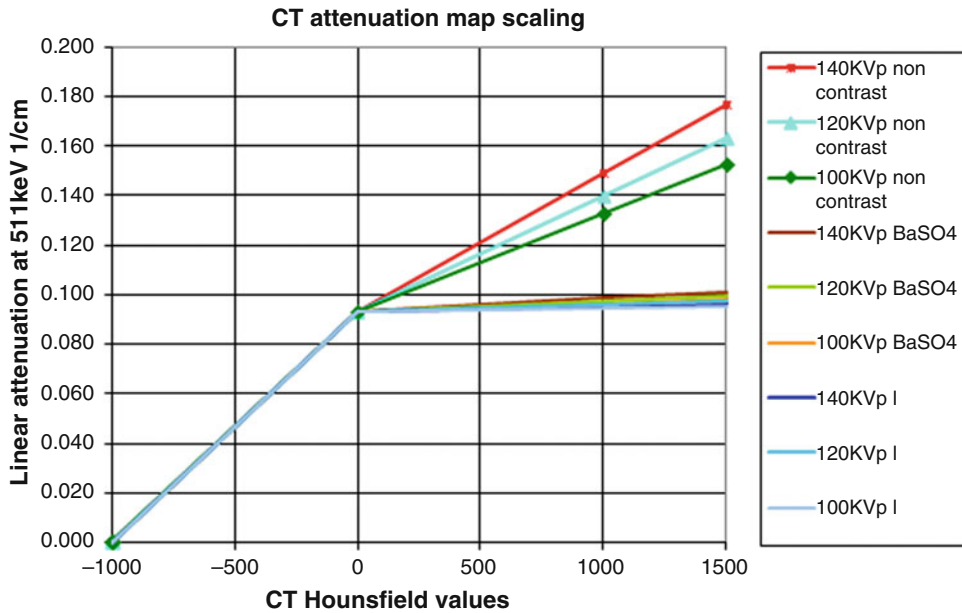


Fig. 3.2 Bilinear transformation to map CT numbers to PET attenuation coefficients at different x-ray tube energies. The graph also shows other transformations that are used when oral or intravenous contrast is used

CT when the patient holds his or her breath at normal expiration, or while the patient breathes shallowly, the CT images best align with the PET images, thereby largely reducing the magnitude of the mismatch effect [39, 42]. Alternatively, computing an average CT scan from multiple CT scans that have been acquired at different phases of the respiratory cycle can be used to mimic the average position captured during PET imaging [43, 44]. Respiratory motion is currently an active research topic in PET/CT imaging particularly because of its effects on radiation treatment planning. By accurately tracking the extent and trajectory of respiratory motion, the treatment plan can be improved by conforming the radiation field to the underlying tumor motion while sparing healthy tissues.

In addition to the mismatch between PET and CT, respiratory motion also blurs the PET image which reduces the measured activity concentration in areas of interest that are moving, such as lung tumors. Both of these effects have prompted manufacturers to develop motion tracking and suppression techniques that are collectively

referred to as four-dimensional (4D) PET/CT. With 4D PET/CT, the acquired PET data are divided into multiple bins (usually 6–10 bins) depending on the phase or amplitude of the breathing cycle. Similarly, CT images are generated at the same temporal points as those at which the PET images were constructed. Each CT image is then used to properly attenuate its corresponding PET image. The resultant PET/CT image sets are then registered to one another and summed to generate a single PET/CT image set that is devoid of motion and mismatch artifacts. To track the breathing motion, several devices are now available from PET/CT manufacturers. The devices depend on either video cameras (such as the real-time position management system by Varian) or respiratory bellows (such as those from Anzai Medical Systems) to track and record a patient's breathing cycle. The complete set of software and hardware components necessary to acquire and process 4D PET/CT data is now available from all PET/CT manufacturers on different scanner models and can be purchased as an option on these systems.

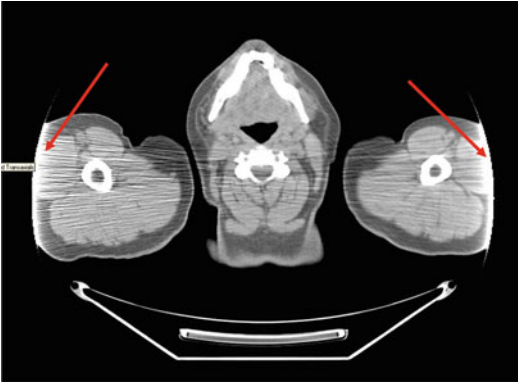


Fig. 3.3 A CT scan of a 145-kg man imaged with arms up. Arrows show truncation artifacts

Another technical problem that is encountered in PET/CT imaging is the difference in the size of the FOV of the CT and PET scanners, resulting in so-called truncation artifacts. Truncation artifact encompasses two forms of error. The first is encountered when imaging a large patient whose cross section extends beyond the FOV of the CT scan (typically a diameter of 50 cm), thus producing severe truncation at the edges of the reconstructed CT images (Fig. 3.3). The second is a result of missing attenuation data resulting from the difference in the FOV size between the PET (typically having an FOV with a diameter of 70 cm) and CT images. The first error is manifested as streaking artifacts at the edge of the CT image, thus causing an artificial overestimation of the attenuation coefficients used in PET as well as degrading the quality of the CT image. The second error results in uncorrected PET data around the periphery of the PET FOV. The two errors have been shown to affect the quantitative and qualitative accuracy of PET images [45, 46]. One way of minimizing these errors is by scanning the patient, in both the CT and PET positions, with the arms raised above the head, thereby reducing the cross-sectional dimension of the patient. This scanning position, however, is very uncomfortable for most patients and increases the likelihood of involuntary movement during the relatively long PET imaging session. Furthermore, scanning patients with their arms up strains the shoulder muscles, which might alter the accumulation of FDG in this region.

Another approach which is currently implemented on all commercially available PET/CT scanners, is to artificially increase the CT reconstructed FOV to match that of the PET. This process can be achieved in different ways, one of which is based on the assumption that the total attenuation per projection is the same independent of the angle at which it was acquired. That is, if all of the attenuation values are summed, that total should be the same regardless of the angle of the projection, as if the CT scanner measured just one huge voxel. Using this assumption, the missing attenuation from truncated projections can be estimated from projections that do not suffer from truncation. This process will result in artificially generated CT attenuation values in areas of the image where such values were not previously recorded. The accuracy of these generated values largely depends on the underlying estimation process. However, because in the majority of the cases the truncated areas are soft tissue, the estimation process results in relatively little error in CT attenuation values. Different proprietary names are given to this process by manufacturers, such as WideView or AC Plus. The scanner operator should preselect the extended FOV option during image reconstruction to ensure that there is no truncation between the PET and CT.

Recent Advances in PET/CT Imaging

Several advances in PET/CT imaging have been achieved since the first edition of this book chapter. PET image quality has improved dramatically, particularly with regard to image resolution, sensitivity, and signal-to-noise ratio. A description of each of the principle means by which the field has advanced to its current state follows.

3D Imaging and Increased Scanner Sensitivity

PET is intrinsically a three-dimensional (3D) imaging modality, replacing physical collimation required for single photon imaging with electronic collimation. Historically, most PET imaging

was performed in two-dimensional (2D) mode, wherein lead septa were placed between the planes of detector elements primarily to reduce scattering photons from being detected. The result was better reconstructed image quality than was possible in the absence of the septa. 2D imaging was also preferred over 3D imaging because of the complexity of 3D image reconstruction algorithms, even though 2D imaging requires more administered activity to obtain adequate count rates, and 3D has roughly a five-fold greater sensitivity. This situation changed in the middle of the first decade of 2000 with the development of new scatter correction techniques and faster and more efficient 3D reconstruction algorithms. Those advances allowed 3D imaging to become the predominant mode of PET data acquisition. The advancement has convinced the manufacturers of PET/CT scanners to abandon 2D imaging altogether. Today, none of the manufacturers of PET/CT scanners are designing new systems that are capable of 2D imaging.

More recently, and in an effort to further increase scanner sensitivity, some manufacturers have increased the axial FOV of the PET system. PET scanners have historically had axial FOV extents of about 15–16 cm, as they were primarily used for brain imaging. Oncologic applications, requiring whole-body imaging, dominate the current demand for PET cameras and thus the value of a longer axial FOV is greater. Today, two of the three major manufacturers provide PET scanners with axial FOV extents longer than 16 cm. All scanners from Philips have axial FOVs of 18 cm. Siemens offers an option called True V on their scanners that extends the axial FOV from 16.2 cm to 21.6 cm, which improves the sensitivity of the scanner by approximately 80% as well as enabling the acquisition of a whole-body scan to be accomplished with fewer bed positions, and hence, shorter time period.

Iterative Reconstruction Algorithms

Originally, PET images were reconstructed using filtered back projection (FBP) techniques similar to single-photon and CT imaging. With the adoption of 3D imaging, FBP was extended to 3D

with the work of Kinahan and Rogers [47] and the introduction of the reprojection algorithm. Statistically based expectation maximization iterative reconstruction techniques were developed for 2D PET image reconstruction and improved the reconstructed image quality compared with that from FBP. These reconstruction algorithms, however, only gained wider acceptance in clinical practice with the introduction of their accelerated version known as ordered subset expectation maximization (OSEM), which was introduced by Hudson and Larkin in 1994. One of the advantages of the iterative reconstruction techniques is their ability to model various aspects of the imaging chain (such as attenuation, scatter, and normalization) during the reconstruction process. This in turn improves the quality of the reconstructed image while maintaining the Poisson nature of its counting statistics in the reconstructed image. More recently a fully 3D version of the OSEM iterative reconstruction algorithm that incorporates corrections for randoms events, scatter events, and attenuation has been developed [48, 49]. In 2006, this algorithm was improved by including corrections for the detector spatial response function resulting in a nearly constant resolution across the transverse FOV of the PET scanner [50]. The point spread function (PSF) of a PET scanner varies within the FOV. Photons emanating from the center of the FOV are normally incident upon the detectors. The obliquity of the path of the annihilation photons with respect to the detector elements is greater when the origin of the photons is closer to the periphery of the FOV. By measuring this variability and then modeling the PSF, improved and nearly uniform spatial resolution can be achieved throughout the FOV. Different forms of this algorithm are now provided by all manufacturers on their respective PET/CT scanners under different proprietary names such as HD or Sharp IR.

Time-of-Flight Imaging

The availability of fast scintillators with high-stopping power such as cerium-doped lutetium

oxyorthosilicate (LSO) (or other lutetium-based detectors such as LYSO) has revived interest in the decades-old concept of time-of-flight (TOF) PET [51, 52]. TOF imaging requires the measurement of the difference between the detection times of the two annihilation photons from the annihilation event – hence the need for fast detectors. The difference in detection time is used to calculate the location of the annihilation event along the line of response (LOR) path. This process improves upon conventional PET imaging (non-TOF) where the location of an annihilation event is not known and hence is placed with equal probability anywhere along the LOR during image reconstruction. Unfortunately, the accuracy by which the arrival time of photons can be detected is on the order of several hundred picoseconds, which translates into a spatial uncertainty of approximately 10 cm in the location of the annihilation event. Even though there is still appreciable uncertainty in the location of the event, with this improved information the TOF reconstruction algorithms can significantly improve the reconstructed image. This improvement in image quality is manifest as an increase in the signal-to-noise ratio (SNR) that is proportional to the square root of D/d where D is the diameter of the activity distribution (i.e., of the object being scanned) and d is the spatial uncertainty. Current commercially available PET/CT scanners with TOF capability are equipped with timing resolution that can identify the location of an annihilation event to within 7–10 cm of spatial uncertainty in the scanner's FOV. For a 40-cm diameter uniform distribution of radioactivity (equivalent to an adult patient cross section), the increase in SNR is on the order of 2–2.3. As the TOF resolution improves, the spatial uncertainty decreases and the SNR increases by a larger factor. Furthermore, as the cross section of the object being imaged increases, the improvement in SNR also increases by a large factor. This is a particularly large advantage in image quality for large patients because conventional imaging of this patient population yields inferior quality because of low counting rates, or requires long scanning sessions at the expense of patient comfort.

Currently, all manufacturers of PET/CT scanners have systems with TOF capabilities. Philips was the first manufacturer to provide such a system in 2007 with the introduction of the Gemini Trueflight TF. Siemens and GE then followed suit with the introduction of the Biograph mCT and GE 690, respectively.

PET/MRI

Although this chapter carries PET/CT in its title, a brief description of PET/MRI is necessary to provide a complete picture of the status of hybrid PET systems. In as much as separately acquired CT images were fused with PET studies, separately acquired MRI data have also been fused with PET. The results have been enticing. Since the introduction of PET/CT imaging and its widespread use by the medical imaging community, manufacturers as well as physicians and scientists started thinking about replacing CT with MRI for a PET/MRI hybrid system. The attraction of such a combined system is based upon the high tissue contrast and nonionizing radiation of MRI as compared with CT imaging. PET/MRI has the further advantage of simultaneous acquisition of the two modalities as compared with the contemporaneous, but sequential imaging process in PET/CT. The latter advantage has specific utility for brain imaging when conducting challenge studies where the stimuli and processes being studied are dynamic. On the other hand, the technical challenges of PET/MRI include the lack of photon attenuation information with which to correct the PET data, nonuniformity of the MRI FOV, truncation artifacts resulting from differences in the FOV size between PET and MRI, susceptibility artifacts in MRI, detecting photons in the presence of a strong magnetic field, and most importantly, a clinical application that specifically would benefit from a hybrid PET/MRI as opposed to PET/CT. This last challenge is of particular importance when keeping in mind that PET/CT imaging is mainly used for oncologic whole-body imaging where simultaneous data acquisition might not be of great advantage. Notwithstanding, both Siemens and Philips

have introduced hybrid PET/MRI systems that are commercially available. The Siemens system, named mMR, is a true simultaneous PET/MRI device whereby the PET scanner is integrated within the MRI FOV. To actualize this system, Siemens had to utilize new PET detectors, which are based on avalanche photo diodes that are immune to the effects of magnetic fields. These detectors, however, are not capable of highly precise timing resolution and therefore the mMR system from Siemens is not capable of TOF imaging. Still, this device is the first true PET/MRI system available on the market that is capable of simultaneously acquiring PET and MR images. The system uses advanced MRI acquisition techniques to help in segmenting the MR images into different tissue types that are later transformed into PET attenuation coefficients for attenuation correction.

The system from Philips on the other hand, is based on contemporaneous acquisition of PET and MRI data similar to the PET/CT design. In this system, the two gantries (PET and MRI) are physically separated from one another by about 4.5 m to minimize the effects of the MRI magnetic field on the PET detectors. Additional PET detector magnetic shielding has also been designed to further reduce the magnetic field effects. A patient couch is installed between the two gantries and is designed to move the patient from one scanner to the other while allowing the patient to remain still in the frame of reference of the couch. The minimized effects of the magnetic field on the PET detectors allows Philips to still offer this scanner with TOF capabilities, which is an advantage over the Siemens design. However, the large distance between the two gantries requires room space that is much larger than that needed for a standard PET/CT. The entire PET/MRI room must be shielded to exclude radiofrequency interference as well as to attenuate ionizing radiation.

Currently, GE Healthcare does not offer a PET/MRI system. Their solution to PET/MRI is to provide a transporter that moves the patient between a dedicated PET/CT and an MRI system. The transporter helps keep the patient in the same orientation during the imaging processes of both PET/CT and MRI, thereby ensuring good

image registration without the need to rely on deformable registration algorithms that would be necessary if the patient were to walk from one scanner to the other. The transporter has a pallet that can dock onto the PET/CT and MRI systems without having to move the patient on its couch. During imaging, the patient lies on the pallet and is later transported to the other scanner. One advantage of this approach is that patient utilization of the two scanners is maximized as one scanner need not be idle while the other scanner is being used, which is the case in the Philips design. At the time of this writing, GE Healthcare indicated that they are working on a new simultaneous PET/MRI system that will be available in the next 1–2 years.

The remainder of this chapter discusses the design specifications of PET/CT scanners in general, and of those that are commercially available in particular.

PET/CT Scanner Design

PET/CT scanners are composed of a PET scanner attached to a CT scanner back-to-back with coaxial bores. The combined structure (except for scanner designs from Philips medical systems) is housed in a single gantry. The CT scanner is usually in the front, and the PET device is located behind the CT. The centers of the two tomographs are separated by 60–70 cm axially to allow space for the CT and PET electronics and to minimize cross talk between the CT and PET detectors. This distance is also important to minimize the temperature variations – critical for the stability of the PET detectors – inside the gantry as a result of turning the CT x-ray tube on and off. The patient couch is located in front of the scanner and is used to advance the patient from the CT to the PET FOV. Because the center of the two tomographs is separated by a large distance, the whole patient couch assembly is translated in the axial direction rather than just translating the patient pallet. This is done to minimize the deflection of the pallet because of patient weight as it is extending from the CT to the PET FOV.

Depending on the manufacturer, the individual CT and PET scanner designs can vary considerably. All CT scanners are now multi-slice systems with helical or axial imaging capabilities, and with different rotation speeds, whereas the PET scanners are capable of only 3D imaging, with bismuth germinate (BGO), LSO, or other lutetium-based detectors such as LYSO, and have a different number of slices per axial FOV. The functionality of PET/CT scanners, however, is the same regardless of manufacturer. Typically, a CT localizer (sometimes called a scout view or a topogram) is acquired to ensure proper patient positioning. This is followed by the CT scan, which is used to generate anatomic images and attenuation maps. At the end of the CT scan, the patient couch assembly is advanced from the CT to the PET FOV, where the PET acquisition is initiated. Following the data acquisition and reconstruction, the PET and CT images can be displayed side by side or fused together. The acquisition of PET data followed by CT is also possible on the systems of all manufacturers. Sophisticated image processing algorithms allow the PET and CT data to be displayed at the same anatomic location even though the PET and CT slices have different thicknesses.

The first prototype PET/CT scanner was developed by David Townsend at the University of Pittsburgh in joint collaboration with CTI Inc. (Knoxville, TN). The initial design work began with a grant from the National Cancer Institute in 1995, and the prototype became operational in 1998. The prototype PET/CT scanner was based on a spiral CT scanner, the single-slice Somatom AR.SP (Siemens; Iselin, NJ), mated to a rotating partial-ring positron emission tomograph, the emission computed axial tomography, advanced rotating tomograph scanner. Both the PET and CT components were mounted on the same assembly with the PET components on the reverse side of the rotating support of the CT scanner. Both scanners were housed inside a single gantry with the centers of the two tomographs offset by 60 cm in the axial direction, allowing a dual-modality examination range of only 100 cm. The design specifics and the first PET/CT images

produced on this prototype scanner can be found elsewhere [53]. The widespread recognition of the importance of imaging anatomy and function together, led by the studies performed on this prototype PET/CT scanner, created a demand for combined PET/CT scanners for imaging cancer in the medical community and stimulated intense commercial activity.

Currently there are three main manufacturers of PET/CT scanners: GE Healthcare, Siemens Medical Solutions, and Philips Medical Systems. Each manufacturer has three scanner models categorized in three tier levels – entry, intermediate, and advanced. GE offers the Optima 560, Discovery 600, and Discovery 690, respectively. Siemens offers the Biograph TruePoint, Biograph mCT 20 Excel, and Biograph mCT, respectively. Philips offers the Gemini TF PET/CT, the Gemini TF Big Bore PET/CT, and the Ingenuity TG PET/CT, respectively.

GE Healthcare PET/CT Scanners

Optima 560

The Optima 560 is the entry level PET/CT scanner from GE Healthcare. The major design considerations of this scanner are the following: (1) 3D-only system, which is a departure from the offering GE used to have on their previous scanners that were capable of both 2D and 3D imaging. (2) The PET system is based on BGO detectors. (3) It has 12,288 detector elements of $4.7 \times 6.3 \times 30$ mm arranged in four rings of 6×8 detectors. (4) PET axial FOV of 15.7 cm resulting in 47 slices each with a 3.27-mm thickness. (5) A transaxial FOV and a patient port of 70 cm. (6) The CT component comes in 8 and 16 slices with the smallest slice thicknesses equal to 1.25 and 0.625 mm, respectively. (7) Rotation as fast as 0.5 s per revolution. (8) The x-ray tube has a maximum power of 53 kW. (9) The maximum current output at 120 kV is 440 mA. (10) The weight of the scanner, including the couch, is 5,200 kg, and its dimensions are 225 cm (W), 146 cm (D), and 193 cm (H). Performance

characteristics of the Optima 560 PET/CT can be found elsewhere [54].

Discovery 600

The Discovery 600 is the intermediate PET/CT offering from GE Healthcare. This system is similar to the Optima 560 except that it has additional capabilities particularly related to motion compensation techniques. The system has the same PET and CT detector design and configuration and is provided in only 8- and 16-slice CT versions. Additional capabilities of the Discovery 600 are related to the performance characteristics of the PET system resulting in higher sensitivity (9.1 vs. 6.5 cps/kBq) and peak noise equivalent count rate (NECR) performance (76 vs. 54 kcps) when compared with the Optima 560. These are probably achieved by allowing larger coincidence acceptance angles in the axial direction. The Discovery 600 scanner also comes with the ability to reduce the nonstationary resolution behavior of PET scanners along the transverse FOV by modeling the PSF during the image reconstruction process. The system also has the option to allow data acquisition in list mode. The list mode gives the user a greater flexibility in designing protocols to evaluate image quality with different scan times. The Discovery 600 system is configured with an adaptive statistical iterative reconstruction engine for CT data, which allows dose reduction while maintaining the quality of the CT images. The system has the same dimensions as the Optima 560 scanner and the performance characteristics of the PET scanner can be found elsewhere [55].

Discovery 690

The Discovery 690 is the premium PET/CT scanner from GE Healthcare. This system has the same capabilities as the Discovery 600 scanner with the following two major differences: (1) LYSO detectors, and (2) TOF imaging capabili-

ties. The LYSO detector elements are slightly smaller in size than their BGO counterparts with sizes equal to $4.2 \times 6.3 \times 25$ mm arranged in the same manner as in the Discovery 600 and the Optima 560 systems. This configuration results in a total of 13,824 detector elements in the scanner. Because of the difference in detector material (LYSO vs. BGO) the PET performance characteristics of this system are different than the Discovery 600 and the Optima 560. The system sensitivity is 7.0 kcps/kBq while the peak NECR is 130 kcps. The lower energy window setting on this system is similar to all other systems from GE Healthcare and is equal to 425 keV. The overall PET performance characteristics of this system can be found elsewhere [56]. This system is offered with two versions of CT scanners; 16 and 64 slices. The latter is known as volume CT because of its relatively large axial extent of 4 cm.

Siemens Medical Solutions PET/CT Scanners

Biograph TruePoint

The Biograph TruePoint is the entry PET/CT scanner from Siemens Medical Solutions. The major design considerations of this scanner are the following: (1) 3D only PET data acquisition. This is a continuation of the trend that Siemens started in the past with scanners that are septaless and hence only allow 3D imaging. (2) 24,336 LSO detectors arranged in blocks of 13×13 detector elements of $4 \times 4 \times 20$ mm. (3) PET axial FOV of 16.2 cm resulting in 81 slices of 2-mm thickness. (4) A transaxial FOV and a patient port of 70 and 60.5 cm, respectively. (5) The CT component previously came in four different versions allowing for 6, 16, 40 and 64 slices per tube rotation. Now this system is only available with a 16-slice CT scanner. (6) Maximum tube rotation times of 0.6–0.33 s per revolution depending on the CT option purchased. (7) The x-ray tube has a maximum power ranging from 50 to

80 kW also depending on the CT version used. (8) The weight of the scanner ranges from 3,200 to 3,980 kg, also depending on the CT version used. The scanner dimensions are 239 cm (W), 156 cm (D), and 202 cm (H). One upgrade option that is available on this system is an extended axial FOV from 16.2 to 21.6 cm (which Siemens refers to as the True V option). This option drastically improves the overall sensitivity performance of the scanner and represents the largest axial extent of any PET/CT scanner on the market. The other upgrade option is modeling the PSF during the PET image reconstruction, which Siemens refers to as the HD option. This improves the transverse resolution across the FOV. In addition, the scanner has motion management capabilities (both respiratory and cardiac). The performance characteristics of the Biograph scanner with and without the True V option can be found elsewhere [57].

Biograph mCT 20 Excel

The Biograph mCT 20 Excel is the intermediate PET/CT system from Siemens Medical Solutions. This system is similar to the TruePoint scanner except for a few additional software and hardware options. First, the CT portion comes in only a 20-slice CT version. The PET component, on the other hand, has TOF imaging capabilities and respiratory motion management. The combination of TOF and HD imaging (see above) is known as the Ultra HD option by Siemens. The patient port was increased from 70 to 78 cm and the transverse FOV was increased to 70 cm to match the size from other manufacturers. The sensitivity and peak NECR of this system have been optimized and improved over the TruePoint system and are equal to 5.3 cps/kBq and 100 kcps/kBq/cc, respectively. The same parameters of the TruePoint system are 4.2 cps/kBq and 96 kcps/kBq/cc. All measurements are based on a lower energy threshold of 435 keV. This system does not come with the option of extended axial FOV (True V) like the TruePoint system. The performance characteristics of this scanner can be found elsewhere [58].

Biograph mCT

The Biograph mCT is the top of the line PET/CT scanner from Siemens Medical Solutions. It combines the flexibility of other scanners by Siemens with respect to different CT slice options, TOF, and motion mitigation options for PET. The system has the same design features as the mCT 20 Excel with respect to patient port and transaxial FOV size. CT slice options available on this system are 40, 64 and 128. For the 128-slice option, the x-ray tube is rated at 100 kW. This system also comes with a True V option and has list mode imaging capabilities. This last feature (list mode), which allows greater flexibility for rebinning the acquired data, is only available on this scanner from Siemens. The performance characteristics of this scanner with and without True V option can be found elsewhere [59].

Philips Medical Systems PET/CT Scanners

The Philips Medical Systems PET/CT scanners are all based on an open design which is a departure from the standard integrated PET and CT systems within a single gantry (Fig. 3.4). The open design has a 30-cm gap between the PET and CT scanners. This distance can be further increased to 88 cm if needed. This design feature maximizes patient acceptance and comfort and allows easy access to the patient during the time of examinations. Philips Medical Systems was the first manufacturer to introduce a TOF PET/CT system to the market. In this regard, all PET/CT scanner models from Philips are TOF-capable and have a timing resolution of 495 ps. The “TF” in the name of all their scanner models captures this capability.

Gemini TF

The Gemini TF is the entry-level PET/CT system from Philips Medical Systems. Other design features of the Gemini TF system include: (1) 3D only imaging capabilities. (2) 28,336 LYSO



Fig. 3.4 Open PET/CT scanner design from Philips Medical Systems (a) compared with a conventional closed system (b). The conventional design shown is for the GE Healthcare Discovery 600

detector elements of $4 \times 4 \times 22$ mm arranged in a continuous pixilated array. (3) PET axial FOV of 18 cm resulting in 91 slices of 2-mm thickness. This is the largest standard axial FOV extent on a commercial PET/CT scanner excluding the True V option from Siemens. (4) A transaxial FOV and a patient port of 67.6 and 70 cm, respectively. (5) The CT component comes in 16- and 64-slice options with the thinnest slices being 0.6 and 0.5 mm, respectively. (6) Rotation times of 0.4 s per revolution for both CT options. (7) Maximum x-ray tube output of 60 kW. (8) Maximum current of 500 mA. (9) The weight of the Gemini TF including the couch is 4,140 kg for the 16-slice CT option and 4,200 kg for the 64-slice option. The scanner dimensions are 225 cm (W), 549 cm (D), and 213 cm (H). Although this is an entry-level system, the Gemini TF has several options allowing it to compete with the highest tier PET/CT systems. Options available for this system are: Motion mitigation techniques and list mode acquisition. The sensitivity of the system is 7.1 cps/kBq while the peak NECR is 110 kcps/kBq measured at a lower energy discriminator of 440 keV. The performance characteristics of the Gemini TF scanner can be found elsewhere [60].

Gemini TF Big Bore

The Gemini TF Big Bore system is identical to the Gemini TF except that the patient port has

been widened to 85 cm. This system is specifically designed to accommodate radiation oncology patients who need to be positioned in specific orientations to accommodate treatment plans. To allow for the enlarged patient port, the manufacturer needed to redesign some of the external shielding of the scanner and thus slightly modified the system performance. The system sensitivity of the big bore scanner is 6.6 cps/kBq while the peak NECR is 90 kcps/kBq when both are measured at a lower energy discriminator of 460 keV. The scanner dimensions and weight are slightly different than the Gemini TF. The CT scanner on this model comes only with 16 slices. All other features and performance characteristics are similar to the Gemini TF.

Ingenuity TF

The Ingenuity TF scanner is the high-end PET/CT scanner from Philips Medical Systems. The PET system design and performance characteristics of this scanner are identical to those of the Gemini TF. The CT components, however, are different. The Ingenuity TF has a CT scanner that is based on the Ingenuity platform, which is capable of acquiring 128 slices per rotation compared with the 16- or 64-slice options of the Brilliance CT platform available on the Gemini scanner. The 128 slices are achieved through wobbling the x-ray focal spot during data

acquisition or what Philips refers to as the Ingenuity data acquisition and sampling technique. The x-ray tube on the Ingenuity platform is rated at 80 kW compared with the 60 kW of the Brilliance platform. In addition, the Ingenuity TF PET/CT system has optimized CT and PET reconstruction engines that allow reducing the patient dose without affecting image quality (CT optimization), as well as reducing the reconstruction time of the TOF data (PET optimization). All other features and performance characteristics are similar to the Gemini TF.

References

1. IMV Medical Information Division. PET market summary report. <http://www.imvinfo.com/index.aspx?sec=pet&sub=dis&itemid=200076>. 2008.
2. Phelps ME, Huang SC, Hoffman EL, et al. Tomographic measurement of local cerebral glucose rate in humans with (F-18)2-fluoro-2-deoxy-D-glucose: validation of method. *Ann Neurol*. 1979;6(5):371–88.
3. Huang SC, Phelps ME, Hoffman EJ, et al. Noninvasive determination of local cerebral metabolic rate of glucose in man. *Am J Physiol*. 1980;238(1):E69–82.
4. Smith TA. FDG uptake, tumor characteristics and response to therapy: a review. *Nucl Med Commun*. 1988;19(2):97–105.
5. Delbeke D. Oncological applications of FDG-PET imaging: brain tumors, colorectal cancer, lymphoma and melanoma. *J Nucl Med*. 1999;40(4):591–603.
6. Gambhir SS, Czernin J, Schwimmer J, et al. A tabulated summary of the FDG-PET literature. *J Nucl Med*. 2001;42(5):1S–93.
7. Bailey DL. Transmission scanning in emission tomography. *Eur J Nucl Med*. 1998;25:774–87.
8. Zaidi H, Hasegawa B. Determination of the attenuation map in emission tomography. *J Nucl Med*. 2003;44(2):291–315.
9. Meikle SR, Dahlbom M, Cherry SR. Attenuation correction using count-limited transmission data in positron emission tomography. *J Nucl Med*. 1993;34:143–50.
10. Xu M, Cutler P, Luk W. An adaptive local threshold segmented attenuation correction method for whole-body PET imaging. *IEEE Trans Nucl Sci*. 1996;43:331–6.
11. Bettinardi V, Pagani E, Gilardi M. An automatic classification technique for attenuation correction in positron emission tomography. *Eur J Nucl Med*. 1999;26:447–58.
12. Bengel FM, Ziegler SI, Avril N, et al. Whole-body positron emission tomography in clinical oncology: comparison between attenuation corrected and uncorrected images. *Eur J Nucl Med*. 1997;24:1091–8.
13. Wahl RL. To AC or not to AC: that is the question. *J Nucl Med*. 1999;40:2025–8.
14. Diederichs CG. Prospective comparison of FDG-PET of pancreatic tumors with high end spiral CT and MRI. *J Nucl Med*. 1998;39(5):81.
15. Eubank WB, Mankoff DA, Schmeidl UP. Imaging of oncologic patients: benefit of combined CT and FDG-PET in the diagnosis of malignancy. *Am J Roentgenol*. 1998;171:1103–10.
16. Wahl RL, Quint LE, Greenough RL, et al. Staging of mediastinal non-small cell lung cancer with FDG-PET, CT and fusion images: preliminary prospective evaluation. *Radiology*. 1994;191(2):371–7.
17. Wahl RL, Quint LE, Cieslak RD, et al. “Anatometabolic” tumor imaging: fusion of FDG-PET with CT or MRI to localize foci of increased activity. *J Nucl Med*. 1993;34(7):1190–7.
18. Vanteenkiste JF, Stroobants SG, Dupont PJ, et al. FDG-PET scan in potentially operable non-small cell lung cancer: Do anatometabolic PET-CT fusion images improve the localization of regional lymph node metastases? The Leuven Lung Cancer Group. *Eur J Nucl Med*. 1998;25(11):1495–501.
19. Woods RP, Cherry SR, Mazziotta JC. Rapid automated algorithm for aligning and reslicing PET images. *J Comput Assist Tomogr*. 1992;16(4):620–33.
20. Kinahan PE, Townsend DW, Beyer T, et al. Attenuation correction for a combined 3D PET/CT scanner. *Med Phys*. 1998;25:2046–53.
21. Hany TF, Steinert HC, Goerres GW, et al. PET diagnostic accuracy: improvement with in-line PET-CT system: initial results. *Radiology*. 2002;225(2):575–81.
22. Israel O, Mor M, Gaitini D, et al. Combined functional and structural evaluation of cancer patients with a hybrid camera-based PET/CT system using F-18-FDG. *J Nucl Med*. 2002;43(9):1129–36.
23. Cohade C, Osman M, Leal J, et al. Direct comparison of FDG-PET and PET-CT imaging in colorectal cancer. *J Nucl Med*. 2002;43(Suppl 5):78.
24. Freudenberg LS, Antoch G, Mueller SP, et al. Preliminary results of whole-body FDG-PET/CT in lymphoma. *J Nucl Med*. 2002;43(Suppl 5):106.
25. Yeung HW, Schoder H, Larson SM. Utility of PET/CT for assessing equivocal PET lesions in oncology: initial experience. *J Nucl Med*. 2002;43(Suppl 5):115.
26. Bar-Shalom R, Keidar Z, Guralnik L, et al. Added value of fused PET/CT imaging with FDG in diagnostic imaging and management of cancer patients. *J Nucl Med*. 2002;43(Suppl 5):117.
27. Mah K, Caldwell CB, Ung YE, et al. The impact of 18F-FDG-PET on target and critical organs in CT-based treatment planning of patients with poorly defined non-small-cell lung carcinoma: a prospective study. *Int J Radiat Oncol Biol Phys*. 2002;52(2):339–50.
28. Erdi YE, Rosenzweig K, Erdi AK, et al. Radiotherapy treatment planning for patients with non-small-cell lung cancer using positron emission tomography (PET). *Radiother Oncol*. 2002;62:51–60.

29. Mutic S, Grigsby PW, Low DA, et al. PET-guided three-dimensional treatment planning of intracavitary gynecologic implants. *Int J Radiat Oncol Biol Phys.* 2002;52(4):1104–10.
30. Dizendorf E, Ciernik IF, Baumert B, et al. Impact of integrated PET CT scanning on external beam radiation treatment planning. *J Nucl Med.* 2002;43(Suppl 5):118.
31. Goerres GW, Hany TF, Kamel E, et al. Head and neck imaging with PET and PET/CT: artifacts from dental metallic implants. *Eur J Nucl Med Mol Imag.* 2002;29(3):367–70.
32. Goerres GW, Ziegler SI, Burger C, et al. Artifacts at PET and PET/CT caused by metallic hip prosthetic material. *Radiology.* 2003;226(2):577–84.
33. Antoch G, Freudenberg LS, Egelhof T, et al. Focal tracer uptake: a potential artifact in contrast-enhanced dual-modality PET/CT scans. *J Nucl Med.* 2002;10:1339–42.
34. Dizendorf EV, Treyer V, von Schulthess GK, et al. Application of oral contrast media in coregistered positron emission tomography-CT. *AJR.* 2002;179(2):477–81.
35. Cohade C, Osman M, Nakamoto Y, et al. Initial experience with oral contrast in PET/CT: phantom and clinical studies. *J Nucl Med.* 2003;44(3):412–6.
36. Arttoch G, Freudenberg LS, Stattaus J, et al. A whole-body positron emission tomography-CT: optimized CT using oral and IV contrast materials. *AJR.* 2002;179(6):1555–60.
37. Mawlawi O, Macapinlac H, Erasmus J, et al. Transformation of CT numbers to PET attenuation factors in the presence of iodinated IV contrast. *Eur J Nucl Med Mol Imag.* 2002;29:S108.
38. Goerres GW, Burger C, Kamel E, et al. Respiration-induced attenuation artifact at PET/CT: technical considerations. *Radiology.* 2003;226(3):906–10.
39. Goerres GW, Kamel E, Heidelberg TNH, et al. PET-CT image co-registration in the thorax: influence of respiration. *Eur J Nucl Med Mol Imag.* 2002;29(3):351–60.
40. Blodgett T, Beyer T, Antoch G, et al. The effect of respiratory motion on PET/CT image quality. *J Nucl Med.* 2002;43(Suppl 5):209.
41. Chin BB, Nakamoto Y, Kraitichman DL, et al. Quantitative differences in F-18 FDG uptake due to respiratory motion in PET CT: attenuation correction using CT in end inspiration and end expiration versus Ge-68 correction. *J Nucl Med.* 2002;43(Suppl 5):210.
42. Goerres GW, Kamel E, Seifert B, et al. Accuracy of image coregistration of pulmonary lesions in patients with non-small cell lung cancer using an integrated PET/CT system. *J Nucl Med.* 2002;43(11):1469–75.
43. Pan T, Mawlawi O, Nehmeh SA, et al. Attenuation correction of PET images with respiration-averaged CT images in PET/CT. *J Nucl Med.* 2005;46(9):1481–7.
44. Pan T, Mawlawi O, Luo D, et al. Attenuation correction of PET cardiac data with low-dose average CT in PET/CT. *Med Phys.* 2006;33:3931–8.
45. Carney J, Townsend DW, Kinahan PE, et al. CT-based attenuation correction: the effects of imaging with the arms in the field of view. *J Nucl Med.* 2001;42(Suppl 5):211.
46. Cody D, Mawlawi O, Forster K. Preliminary study of CT transmission truncation and beam hardening artifacts on quantitative PET activity. *Semin Nucl Med* (accepted abstract). *J Nucl Med* 2003;44(Suppl 5):273.
47. Kinahan PE, Rogers JG. Analytic 3d image-reconstruction using all detected events. *IEEE Trans Nucl Sci.* 1989;36(1):964–8.
48. Comtat C, Bataille F, Michel C, et al. OSEM-3D reconstruction strategies for the ECAT HRRT. *IEEE Nuclear Science Symposium Conference Record* 2004; vol 6, p. 3492–6.
49. Liu X, Comtat C, Michel C, et al. Comparison of 3-D reconstruction with 3D-OSEM and with FORE+OSEM for PET. *IEEE Trans Med Imag.* 2001;20(8):804–14.
50. Panin VY, Kehren F, Michel C, et al. Fully 3-D PET reconstruction with system matrix derived from point source measurements. *IEEE Trans Med Imag.* 2006;25(7):907–21.
51. Mullani N, Wang W, Hartz P, et al. Sensitivity improvement of TOFPET by the utilization of the inter-slice coincidences. *IEEE Trans Nucl Sci.* 1982;29(1):479–83.
52. Budinger TF. Time-of-flight positron emission tomography: status relative to conventional PET. *J Nucl Med.* 1983;24:73–8.
53. Beyer T, Townsend DW, Brun T, et al. A combined PET/CT scanner for clinical oncology. *J Nucl Med.* 2000;41(8):1369–79.
54. GE Optima PET/CT 560 data sheet, 2011.
55. De Ponti E, Morzenti S, Guerra L, et al. Performance measurements for the PET/CT Discovery-600 using NEMA NU 2–2007 standards. *Med Phys.* 2011;38(2):968–74.
56. Kemp B, Williams J, Ruter R, et al. Performance measurements of a whole body PET/CT system with time-of-flight capability. *J Nucl Med.* 2009;50(Suppl 2):1546P.
57. Jakoby BW, Bercier Y, Watson CC, et al. Performance characteristics of a new LSO PET/CT scanner with extended axial field-of-view and PSF reconstruction. *IEEE Trans Nucl Sci.* 2009;56(3):633–9.
58. Siemens Biograph mCT 20 Excel data sheet, 2011.
59. Jakoby BW, Bercier Y, Conti M, et al. Performance investigation of a time-of-flight PET/CT scanner. *IEEE Nuclear Science Symposium Conference Record* 2008; Dresden, Germany p. 3738–43.
60. Surti S, Kuhn A, Werner ME, et al. Performance of Philips Gemini TF PET/CT scanner with special consideration for its time-of-flight imaging capabilities. *J Nucl Med.* 2007;48(3):471–80.